Q. J. R. Meteorol. Soc. (2003), **129**, pp. 1565–1588 doi: 10.1256/qj.02.186

A comparison of model-simulated trends in stratospheric temperatures

By K. P. SHINE[1]*, M. S. BOURQUI[1], P. M. de F. FORSTER[1], S. H. E. HARE[1], U. LANGEMATZ[2], P. BRAESICKE[3], V. GREWE[4], M. PONATER[4], C. SCHNADT[4], C. A. SMITH[5], J. D. HAIGH[5], J. AUSTIN[6], N. BUTCHART[6], D. T. SHINDELL[7], W. J. RANDEL[8], T. NAGASHIMA[9], R. W. PORTMANN[10], S. SOLOMON[10], D. J. SEIDEL[11], J. LANZANTE[12], S. KLEIN[12], V. RAMASWAMY[12] and M. D. SCHWARZKOPF[12]

[1]*Department of Meteorology, The University of Reading, UK*
[2]*Freie Universität Berlin, Germany*
[3]*Department of Chemistry, University of Cambridge, UK*
[4]*DLR, Oberpfaffenhofen, Germany*
[5]*Imperial College of Science Technology and Medicine, London, UK*
[6]*Met Office, Bracknell, UK*
[7]*NASA Goddard Institute for Space Studies, New York, USA*
[8]*National Center for Atmospheric Research, Boulder, USA*
[9]*National Institute for Environmental Studies, Ibaraki, Japan*
[10]*NOAA Aeronomy Laboratory, Boulder, USA*
[11]*NOAA Air Resources Laboratory, Silver Spring, USA*
[12]*NOAA Geophysical Fluid Dynamics Laboratory, Princeton, USA*

(Received 10 September 2002; revised 4 December 2002)

SUMMARY

Estimates of annual-mean stratospheric temperature trends over the past twenty years, from a wide variety of models, are compared both with each other and with the observed cooling seen in trend analyses using radiosonde and satellite observations. The modelled temperature trends are driven by changes in ozone (either imposed from observations or calculated by the model), carbon dioxide and other relatively well-mixed greenhouse gases, and stratospheric water vapour.

The comparison shows that whilst models generally simulate similar patterns in the vertical profile of annual- and global-mean temperature trends, there is a significant divergence in the size of the modelled trends, even when similar trace gas perturbations are imposed. Coupled-chemistry models are in as good agreement as models using imposed observed ozone trends, despite the extra degree of freedom that the coupled models possess.

The modelled annual- and global-mean cooling of the upper stratosphere (near 1 hPa) is dominated by ozone and carbon dioxide changes, and is in reasonable agreement with observations. At about 5 hPa, the mean cooling from the models is systematically greater than that seen in the satellite data; however, for some models, depending on the size of the temperature trend due to stratospheric water vapour changes, the uncertainty estimates of the model and observations just overlap. Near 10 hPa there is good agreement with observations. In the lower stratosphere (20–70 hPa), ozone appears to be the dominant contributor to the observed cooling, although it does not, on its own, seem to explain the entire cooling.

Annual- and zonal-mean temperature trends at 100 hPa and 50 hPa are also examined. At 100 hPa, the modelled cooling due to ozone depletion alone is in reasonable agreement with the observed cooling at all latitudes. At 50 hPa, however, the observed cooling at midlatitudes of the northern hemisphere significantly exceeds the modelled cooling due to ozone depletion alone. There is an indication of a similar effect in high northern latitudes, but the greater variability in both models and observations precludes a firm conclusion.

The discrepancies between modelled and observed temperature trends in the lower stratosphere are reduced if the cooling effects of increased stratospheric water vapour concentration are included, and could be largely removed if certain assumptions were made regarding the size and distribution of the water vapour increase. However, given the uncertainties in the geographical extent of water vapour changes in the lower stratosphere, and the time period over which such changes have been sustained, other reasons for the discrepancy between modelled and observed temperature trends cannot be ruled out.

KEYWORDS: Greenhouse gases Ozone depletion Stratospheric water vapour Temperature trends

1. INTRODUCTION

The stratosphere has been cooling over recent decades and the causes of this trend have been the subject of scrutiny using a wide variety of numerical models (see e.g. WMO 1999; Ramaswamy *et al.* 2001; and references therein).

* Corresponding author: Department of Meteorology, University of Reading, Earley Gate, Reading, Berkshire RG6 6BB, UK. e-mail: k.p.shine@reading.ac.uk

WMO (1999) concluded that stratospheric ozone depletion was the dominant cause of temperature trends in the lower stratosphere, while ozone depletion and increases in the more well-mixed greenhouse gases both contributed significantly in the middle and upper stratosphere. It also concluded that there was little evidence that changes in tropospheric climate and sea surface temperatures (SSTs) have played a significant role in stratospheric temperature trends.

There have been three major developments in this area since WMO (1999). First, at the time of WMO (1999) most of the model studies of the impact of ozone changes on stratospheric temperatures had used rather idealized vertical distributions of the ozone change. More refined datasets on the vertical trends in ozone are now in quite widespread use; in addition, more groups have now included the concurrent changes in greenhouse gases in their calculations. Second, several groups have reported simulated temperature trends over recent decades using models with interactive chemistry schemes. Third, there has been significant attention paid to the potential role of changes in stratospheric water vapour on temperature trends.

In the light of these developments, it is necessary to revisit the conclusions of WMO (1999). To quantify the extent to which the observed temperature trends can be attributed to observed constituent changes, it is necessary to establish the degree to which the models reproduce the observed trends.

This paper seeks to improve understanding of the causes of the observed stratospheric temperature trends since about 1980 by bringing together results from many recent studies and presenting them in a common format. This enables a more straightforward comparison between the models, and with observations, than can be achieved by referring to each individual study alone; it allows the identification of common features amongst the models and common discrepancies between the models and observations. The comparison was initiated as part of the World Meteorological Organization's and United Nations Environment Programme's Scientific Assessment of Ozone Depletion 2002 (WMO 2003) where, because of space limitations, only a small subset of the results presented here could be included.

This paper is restricted mainly to an analysis of the vertical profile of the annual- and global-mean trends, but also includes annual- and zonal-mean changes in the lower stratosphere. In section 2, the participating models are presented, along with details of the source of the observed temperature trends that are used here. In section 3, the modelled global-mean trends from a variety of mechanisms are presented, along with a synthesis of these results where they are compared with observations. In section 4, the zonal-mean results are discussed, and in section 5 conclusions are drawn.

2. Participating models and observational datasets

The participating models range in complexity from fixed dynamical heating (FDH) models, through two-dimensional (2-D; latitude–height) models (sometimes with coupled chemistry), through to general-circulation models (GCMs) which use either imposed ozone trends or ozone trends calculated within the model. All the results presented here have either been published or are from experiments using established models. Table 1 lists the contributors to this comparison, together with some details of the models and their abbreviations used in the text. The vertical resolution of the models can be inferred from the symbols used on the figures presented in section 3.

It is emphasized that the comparisons presented here are based on existing simulations that have been performed by the contributing groups, rather than being a strict intercomparison where all groups perform a well-defined set of identical experiments;

TABLE 1. CONTRIBUTORS TO THE MODEL TEMPERATURE TREND COMPARISON

Institute[1]	Contributor	Model and experiment types	Brief details	Relevant references
University of Cambridge, UK *Cambridge*	P. Braesicke	Met Office Unified Model Transient, forced with observed SSTs; no imposed changes in trace gases	2.5° × 3.75° resolution 58 levels, top at 0.1 hPa (approx. 64 km) Modified Cariolle ozone scheme	Braesicke and Pyle (2003)
Freie Universität Berlin, Germany *Berlin*	U. Langematz	Berlin Climate Middle Atmosphere GCM Timeslice Imposed O_3 and ghg changes	T21 (approx. 5.5°) resolution 34 levels, model top at 84 km	Langematz (2000) ozone only results Langematz *et al.* (2003) ozone and CO_2 results
DLR-Institut für Physik der Atmosphäre, Germany *E39C*	V. Grewe C. Schnadt	ECHAM4.L39 (DLR)/CHEM GCM Timeslice Coupled O_3 change	T30 (approx. 4°) resolution 39 levels, model top at 10 hPa (approx. 32 km) Family chemistry model	Hein *et al.* (2001) Schnadt *et al.* (2002)
Imperial College, UK *Imp. Coll.2-D*	C. A. Smith J. D. Haigh	2-D model Timeslice Imposed O_3 and stratospheric H_2O changes	19 latitudes 29 levels, top at 95 km	Smith *et al.* (2001)
Imp. Coll. IGCM		Reading Intermediate GCM Timeslice Imposed stratospheric H_2O changes	T21(approx. 5.5°) resolution 26 levels, model top at 0.1 hPa (approx. 64 km)	Model is Rosier and Shine (2000) Results reported in Smith (2001)
NOAA Geophysical Fluid Dynamics Laboratory, USA *GFDL*	V. Ramaswamy D. Schwarzkopf	SKYHI GCM Timeslice Imposed O_3 and ghg changes	3.6° × 3.0° resolution 40 levels, model top at 80 km	Ramaswamy and Schwarzkopf (2002) The 'Run B' results are used here
NASA Goddard Institute of Space Studies *GISS*	D. Shindell	GISS GCM Transient Coupled O_3 change and imposed ghg change	8° × 10° resolution 23 levels, model top at 0.002 hPa (approx. 85 km) Simplified interactive chemistry	Shindell (2001) Shindell and Grewe (2002)
Met Office, UK *UK Met Office L64*	J. Austin N. Butchart	Met Office Unified Model with Eulerian transport and chemistry Transient Coupled ozone change	2.5° × 3.75° resolution 64 levels, top at 0.01 hPa (approx. 80 km) One simulation with gravity wave drag scheme (GWD), one with Rayleigh friction Family chemistry scheme 13 species/families	Austin (2002)
UK Met Office L49	N. Butchart	Met Office Unified Model Transient Imposed ghg change	2.5° × 3.75° resolution 49 levels, top at 0.1 hPa (approx. 64 km)	Butchart *et al.* (2000)
National Institute for Environmental Studies, Japan *CCSR/NIES*	T. Nagashima	CCSR/NIES GCM Transient Coupled ozone change	T21 (approx 5.5°) resolution 34 levels, model top at 80 km 19 species, 5 families in chemistry scheme	Takigawa *et al.* (1999) Nagashima *et al.* (2002)
NOAA Aeronomy Laboratory, USA *NOAA Aeronomy*	R. W. Portmann S. Solomon	2-D model Timeslice Coupled O_3 and imposed stratospheric H_2O changes	5.1° resolution 56 levels, model top at 112 km Fully coupled-chemistry, breaking gravity-wave and planetary-wave parametrizations	Dvortsov and Solomon (2001)
University of Reading, UK *Reading IGCM*	M. Bourqui S. H. E. Hare	Reading Intermediate GCM Timeslice Imposed O_3 and ghg change	T21(approx. 5.5°) resolution, 26 levels, model top at 0.1 hPa (approx. 64 km)	Model slightly updated from Rosier and Shine (2000)
Reading FDH	P. Forster	Fixed Dynamical Heating Model Timeslice Imposed O_3 and stratospheric H_2O change	18 latitudes, 19 levels, model top at 1 hPa (approx. 48 km) Default code is 10 cm^{-1} narrow band model (NBM), but two GCM schemes (ECHAM and Zhong) used in some runs	Forster *et al.* (2001) for ozone experiments Forster and Shine (2002) for water vapour experiments

[1] Shortened names in italics are used in the text.

'Timeslice' refers to the calculation of temperature trends by carrying out extended integrations of the model for conditions representative of two years and calculating the trend from the difference between these simulations. Transient models perform continuous integrations through the given period. 'ghg' is greenhouse gases. Further details of the coupled-chemistry GCMs can be found in Austin *et al.* (2003). See text for acronyms.

consequently, for example, the time periods for which trends have been calculated vary slightly amongst the groups. A strict intercomparison would have been a formidable exercise amongst such a wide number of model types and different experiments. It will be shown that, despite the differences in experimental design, many common features in the model–observation comparison emerge.

To compare the model-derived temperature trends with observations, we use global measurements of stratospheric temperatures over the period from late 1978 to 1997, based on measurements from the series of operational National Oceanic and Atmospheric Administration (NOAA) satellites and a recent analysis of radiosonde data. This paper neither purports to provide a detailed comparison of observed trends from different data sources, nor attempts to assess the fidelity of the observations or their uncertainties; more information on these aspects can be found in, for example, WMO (1999), Ramaswamy *et al.* (2001; 2002) and in the references to the individual datasets, cited below.

For the satellite trend analyses, data are from the Microwave Sounding Unit (MSU) and the Stratospheric Sounding Unit (SSU). MSU channel 4 provides a measure of the weighted mean temperature in the 150 to 50 hPa layer (approximately 13–22 km, with a maximum contribution near 17 km; Spencer and Christy (1993)). This layer lies in the lower stratosphere over middle to high latitudes; in the tropics it spans the upper troposphere and lower stratosphere. A continuous record is provided by the series of MSU instruments. It is necessary to make adjustments to the time series from each instrument so that they match during periods of overlap; this contributes to the uncertainty in the derived trends. Lower-, middle- and upper-stratospheric temperatures are derived from several SSU channels. SSU data represent temperatures over relatively thick layers, with a vertical resolution of about 10–15 km. A series of original and 'synthetic' channels were derived by Nash and Forrester (1986), using the nadir and off-nadir measurements, to increase the effective vertical resolution. SSU temperature measurements from the series of NOAA satellites have been combined using temporal overlap to generate homogeneous time series, for use in trend analyses (John Nash, personal communication; Ramaswamy *et al.* 2001). Trends are calculated using a standard regression analysis, including proxies for the quasi-biennial oscillation and solar cycle variations (Randel and Cobb 1994); also, two years following the El Chichon and Pinatubo volcanic eruptions were omitted from the time series to remove major volcanic influences (WMO 1999). All plots here include trends from observations with the 2-sigma error bars in these trends. In addition, since each satellite observation represents the temperature of a layer about 10–15 km deep, the vertical 'error' bar on the global-mean plots gives an approximate indication of the layer over which each satellite channel senses temperature.

These fairly deep vertical layers sampled by the MSU and SSU instruments do not allow a detailed examination of the vertical profile of trends; for that purpose we use radiosonde observations which yield height-resolved trends in the lower stratosphere. The radiosonde trend analyses used here are from Lanzante *et al.* (2003a,b; henceforth LKS) who have used a near-globally distributed set of 87 stations; although generally well distributed, the LKS data do not provide nearly as much coverage as either the satellite or the model data, so there is an inherent mismatch, and the number of stations reporting data decreases with height. An advantage of this particular analysis is that extensive efforts have been made to homogenize the data series by examining each station's data series for discontinuities, and using information on day–night differences, the vertical structure of temperature, changes in instrumentation and observing practices, and statistical indicators of abrupt change. However, these adjustments are unlikely to

remove all artifacts. There is evidence that the trends in the tropical lower stratosphere, in particular, are still too negative even after adjustment (Lanzante *et al.* 2003b). For the present purposes, this dataset has one advantage over alternative radiosonde datasets as it includes trends up to 10 hPa, although the quantity and quality of data at pressures lower than 50 hPa diminishes so that the data here should be treated with considerable caution. Linear temperature trend estimates are derived, together with 2-sigma confidence intervals, from monthly temperature anomalies for 1979–97 averaged over 30° latitude bands; note that the analyses differ from that in LKS, as here the data from all stations in a given region are combined to produce the trend analyses, whereas in LKS the data were analysed on a station-by-station basis. For the sake of clarity, the LKS data are only included on selected plots presented here.

It must be re-emphasized that none of the sources of observed temperature trends is ideal. Data from both satellite and sonde require corrections to produce homogeneous series and these corrections are unlikely to be perfect. The sonde data have serious spatial sampling problems that get worse with altitude in the stratosphere. Also, use of linear trends is a simplified metric of actual temperature change, particularly because of the impact of stratospheric volcanic aerosols on the temperature trend series. These uncertainties need to be borne in mind when comparing models with observations, as discrepancies are not necessarily due to model error.

3. Global- and annual-mean results

The vertical profiles of the global- and annual-mean temperature trends derived from the models are subject to uncertainty due to unforced variability in the models, but this is generally small in the global mean as the global-mean stratosphere is close to radiative equilibrium. The 2-sigma variability in the global- and annual-mean temperatures in the GFDL GCM is always less than 0.25 K between 100 hPa and 1 hPa, and is less than 0.15 K in the Berlin and Reading GCMs. An alternative method to characterize the variability comes from the Cambridge GCM results (Braesicke and Pyle 2003). In these calculations the observed time-varying SSTs are imposed, but trace gas concentrations are held fixed; hence the trends in this model are driven either by surface temperature changes or by internal processes. Trends, calculated over two different periods (1980–94 and 1980–99) never exceed 0.12 K decade^{-1} between 100 hPa and 10 hPa. As will be shown, the total simulated trends resulting from the changes in the trace gases generally comfortably exceed these values.

A further consideration is the impact of varying surface and tropospheric conditions on the stratosphere, as these alter the upwelling radiation at the tropopause. Some models discussed here include changes in tropospheric temperatures, others do not. The Cambridge results mentioned above indicate a rather modest effect of such changes. Comparisons between FDH and GCM calculations using the E39C model (see Table 1) indicate that allowing changes to the surface and troposphere, as well as the stratosphere, in the period 1980–90, leads to warming at 100 hPa of a few tenths of a K decade^{-1}, falling to less than 0.05 K decade^{-1} at 10 hPa. However, the E39C experiments include only greenhouse gas increases but no tropospheric cooling effects due to tropospheric aerosols. This will lead to an exaggerated lower-stratospheric warming, but the impact on the vertical profile is indicative of the sign of a real physical mechanism that is not included in FDH calculations or models with fixed SSTs. A related consideration is that even the choice of the tropopause definition has an effect on the modelled lower-stratospheric trends for FDH models (Forster *et al.* 1997).

The observed cooling from the satellite data is included for reference on all plots for individual temperature trend mechanisms, but agreement between model and observations for individual mechanisms should not be expected. The discussion in section 3(e) brings together the information from these individual mechanisms into a coherent overall picture and compares them with observed trends. Note also that the shorthand 'greenhouse gases' is used here to indicate the longer-lived and more well-mixed species of carbon dioxide, methane, nitrous oxide and the halocarbons.

(*a*) *Simulated temperature trends using observed ozone trends*

At the time of WMO (1999), most of the modelling (especially GCM) work had imposed observed total column trends, but had made idealized assumptions about the vertical distribution of those trends. Improved analyses of vertical profiles of ozone change over the period from about 1979 to 1997 (e.g. Randel and Wu 1999; Langematz 2000) have now been used in models to re-examine the temperature trend. Langematz (2000), Rosier and Shine (2000), Ramaswamy and Schwarzkopf (2002) and Langematz *et al.* (2003) all report the impact of using these trends in GCMs, while Smith (2001) reports the impact in a 2-D zonal-mean model. Forster *et al.* (2001) report results from a comparison of several different radiation schemes, using a latitudinally resolved FDH model. All the results reported here use essentially the same observed ozone trends and so allow a quite direct comparison of model behaviour; all the models use the Randel and Wu (1999) trends except for the Berlin model, but the trends used in this are derived from the same ozone dataset. There is clearly uncertainty in our knowledge of the observed ozone trends (see WMO 1999) and also not all the derived trends will be statistically significant. These facts are not important when comparing models, but become significant when the model and observed trends are compared in section 3(e).

Figure 1 shows the vertical profile of the global- and annual-mean temperature trends as a function of pressure. All models have qualitatively the same behaviour with: a peak cooling near 1 hPa exceeding 1 K decade^{-1}; a minimum near 10 hPa with two models even getting a slight warming; and a secondary cooling peak near 80 hPa, of about 0.4 K decade^{-1}. However, there is a significant amount of disagreement between the models in both the magnitude of the cooling and the altitude of the main features, most particularly near 1 hPa. The dominant reasons for these differences seem likely to be the particular radiation codes being used in models (Forster *et al.* 2001; also see the spread in the Reading FDH results in Fig. 1) and the assumed background climatology of ozone (Ramaswamy and Schwarzkopf 2002). It should also be noted that the spread of model results is not obviously related to the model type, as the spread from GCMs is similar to that from the simpler models.

A further contributor to temperature trends in the lower stratosphere comes from increases in tropospheric ozone concentrations; as discussed in WMO (1999), these can act to cool the lower stratosphere by reducing the upwelling radiation from the troposphere in the 9.6 μm band of ozone. Sexton *et al.* (2003), using tropospheric ozone trends derived from a chemical-transport model, found a global-mean cooling of around 0.05 K decade^{-1} at 50 hPa in recent decades. Although smaller than the magnitude of the cooling induced by stratospheric ozone loss, it has probably been sustained over many decades; Sexton *et al.* (2003) estimate the cooling from tropospheric ozone of about 0.5 K over the 20th century. It must be noted that it is difficult to evaluate the ozone increases produced by chemical-transport models, and over recent decades not all regions show evidence for an increase in tropospheric ozone (WMO 1999).

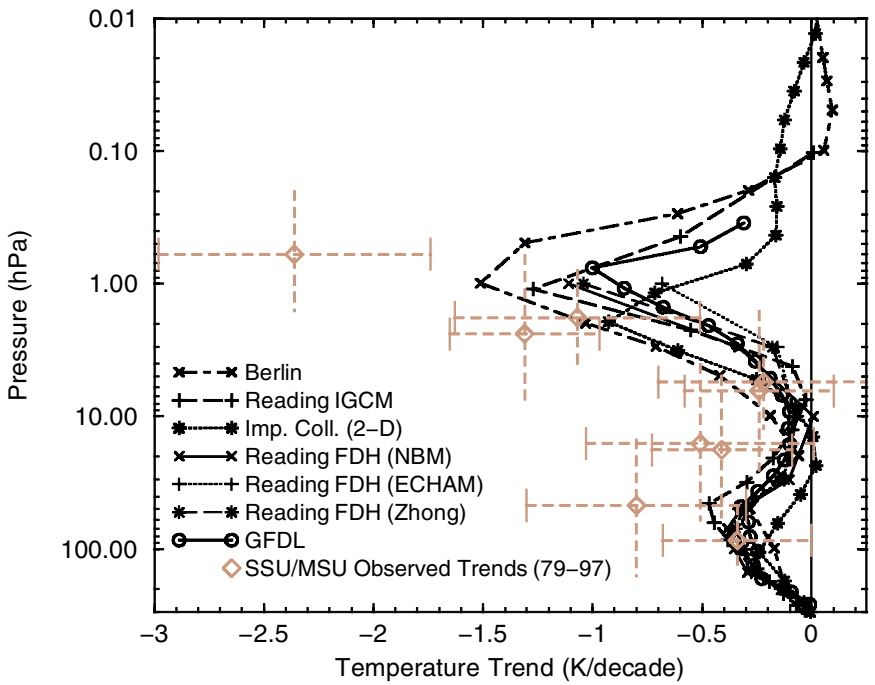

Figure 1. Global- and annual-mean temperature trends for models using imposed height-resolved ozone trends for the period 1979–97. The trends from the Microwave Sounding Unit (MSU) and the Stratospheric Sounding Unit (SSU) are also shown. The 2-sigma error bars in the observations are included; the vertical bars are intended to give the approximate altitude range sensed by the particular satellite channel. Note that the observations are shown here for reference, but it is not expected that ozone trends alone will account for the observed trends. See Table 1 for details of models.

(*b*) *Simulated temperature trends due to increased greenhouse gas concentrations*

Figure 2 shows the vertical profile of the annual- and global-mean temperature changes for trends in greenhouse gas concentrations only (and with those changes not impacting on ozone concentrations). For this case, the time periods over which the greenhouse gas changes were imposed varied amongst the models. This has only a modest impact on the trends. The decadal rate of increase in carbon dioxide has been nearly constant (15 ppmv decade^{-1}) between 1980 and 2000. Reading Narrow Band Model (NBM, see Table 1) FDH calculations indicate that for perturbations of between 10 and 30 ppmv, the cooling per ppmv change in carbon dioxide differs by no more than 4% between 100 hPa and 1 hPa; this indicates that there is no significant nonlinearity, at least from the viewpoint of a purely radiative response.

As with the calculations following imposed ozone changes, there is qualitative agreement among the models of a cooling that generally increases monotonically with height from near-zero at 100 hPa to around 0.8 K decade^{-1} at 1 hPa. Between 100 and 10 hPa there is general agreement among most of the models, but there is considerable divergence around 1 hPa, with almost a factor of four difference between the model with the most cooling (UK Met Office, Butchart *et al.* 2000) and that with the least (Goddard Institute of Space Studies (GISS), Shindell 2001). Given that the greenhouse gas changes are fairly linear and well constrained over this period, this divergence is surprising. It may be related to the ability of individual radiation codes to simulate heating rate changes at these low pressures; Forster *et al.* (2001) compare

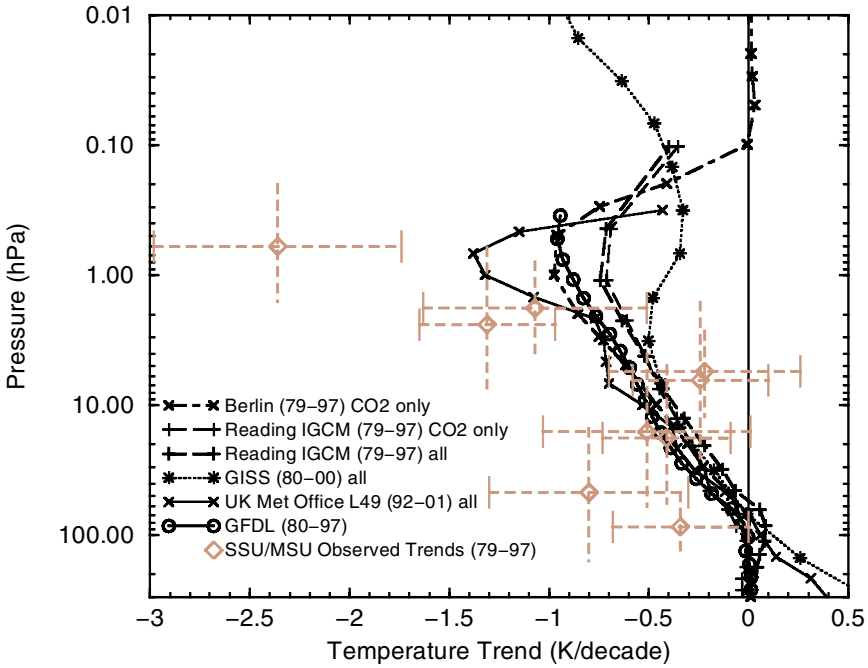

Figure 2. As Fig. 1 but using imposed greenhouse gas trends (it is not expected that greenhouse gas trends alone will account for the observed trends).

FDH temperature trends from three different radiation schemes and show differences of about 15% in the upper stratosphere, which could account for some, but not all, of the spread seen in Fig. 2.

Some of the models here include only changes in carbon dioxide, while others include changes in other greenhouse gases, such as methane, nitrous oxide and various halocarbons. The Reading IGCM results on Fig. 2 indicate the impact of these additional gases. At 1 hPa, these gases enhance the cooling trend due to carbon dioxide alone by about 5%, via increased infrared emission. Lower in the stratosphere the addition of halocarbons, which absorb significantly in the 8–13 μm window region, causes a relative heating; this is because the absorption of upwelling infrared radiation from the troposphere by the halocarbons more than offsets the increased local infrared emission. Ramaswamy *et al.* (1996) have shown that this heating significantly offsets the cooling trend due to carbon dioxide changes alone in the 50–100 hPa layer. The Reading IGCM includes halocarbons other than CFC-11 and CFC-12 as an 'effective' CFC-11 (where the effectiveness is determined by their contribution to radiative forcing relative to CFC-11). More refined calculations using the Reading NBM FDH (not shown) indicate that the heating in the lower stratosphere due to the CFCs is probably exaggerated by about a factor of two in the Reading IGCM, and the heating trend due to the CFCs is around 0.04 K decade^{-1} at 100 hPa. Hence the greenhouse gases other than carbon dioxide have only a modest impact on the modelled temperature trend, and cannot explain the intermodel differences seen in Fig. 2.

(*c*) *Simulated temperature trends due to trends in stratospheric water vapour*

Observations of increases in stratospheric water vapour (e.g. Oltmans *et al.* 2000; Rosenlof *et al.* 2001), which are approximately double those estimated to result from

methane oxidation, have led to renewed interest in the climatic implications (Forster and Shine 1999,2002; Dvortsov and Solomon 2001; Oinas *et al.* 2001; Shindell 2001; Smith 2001; Smith *et al.* 2001).

Two model calculations with idealized water vapour change (i.e. 700 ppbv from a constant stratospheric background of 6000 ppbv) adopted by Forster and Shine (1999) and Oinas *et al.* (2001) are not included here. As noted by Forster and Shine (2002), these idealized changes do not give a reliable indication of actual temperature changes because of the background water vapour that is adopted. Both Oinas *et al.* (2001) and Forster and Shine (2002) demonstrate a strong dependence of a given water vapour perturbation on this background.

A major difficulty in comparing estimates of the temperature trend is uncertainty in the temporal and geographical variation of stratospheric water vapour changes. The only near-global estimates that include the lower stratosphere are from the Halogen Occultation Experiment (HALOE) instrument. Smith *et al.* (2001) report global-mean HALOE trends from 1992 to 1999 ranging from 80 ppbv year^{-1} in the upper stratosphere, decreasing at pressures greater than 20 hPa to 20 ppbv year^{-1} at 50 hPa and to near-zero at 70 hPa. Rosenlof *et al.* (2001) compare results from a variety of sources in northern midlatitudes. Sonde measurements from Boulder (Colorado, USA) for the period 1980–2000 yield trends between 20 and 100 hPa that are approximately constant with height at 45–50 ppbv year^{-1}. HALOE (1992–2000) trends in the same region, on the other hand, drop from 35 ppbv year^{-1} at 20 hPa to slightly negative at 70 hPa; the HALOE values should be treated as somewhat approximate as the trend depends on the end-points chosen in the analysis. Evidence of a longer-term trend (about 50 ppbv year^{-1} since the mid-1950s) is even more limited (Rosenlof *et al.* 2001).

Such differences in water vapour changes are bound to have a severe impact on computed temperature trends. Here, Imperial College uses HALOE data for the period 1992–99, and assumes that trends polewards of 75° (where HALOE does not observe) are the same as at 75°. Reading and NOAA Aeronomy models assume that the Boulder data, with their much more limited spatial coverage but longer time sampling and better lower-stratospheric sensitivity, are globally representative. Reading applies a 50 ppbv year^{-1} trend and NOAA Aeronomy applies a 35 ppbv year^{-1} trend, both throughout the stratosphere.

Figure 3 shows the vertical profile of the global- and annual-mean temperature trends from these models. In the mid-to-upper stratosphere, where water vapour trends are more consistent, the models all produce a cooling of 0.1–0.2 K decade^{-1}. However, in the lower stratosphere there is a large disagreement that reflects the wide divergence in the applied water vapour trends. For example, at 50 hPa there is a factor of three difference in cooling between the models using the HALOE trends (Imperial College) and the Reading model (where the cooling reaches about 0.5 K decade^{-1}); this is broadly consistent with the differences in the applied water vapour trend, but disagreement will also result from the assumptions regarding the background water vapour used in each model, as discussed above, and from differences in the radiation codes (Forster *et al.* 2001). Preliminary results from the GFDL GCM using HALOE water vapour trends (not shown) are in generally good agreement with those from Imperial College for pressures less than 70 hPa.

(*d*) *Simulated temperature trends from coupled-chemistry models*

GCMs coupled to stratospheric chemistry schemes are now in increasing use. Current models include a range of different chemistry schemes ranging from computationally faster but more highly parametrized schemes (Shindell and Grewe 2002) to

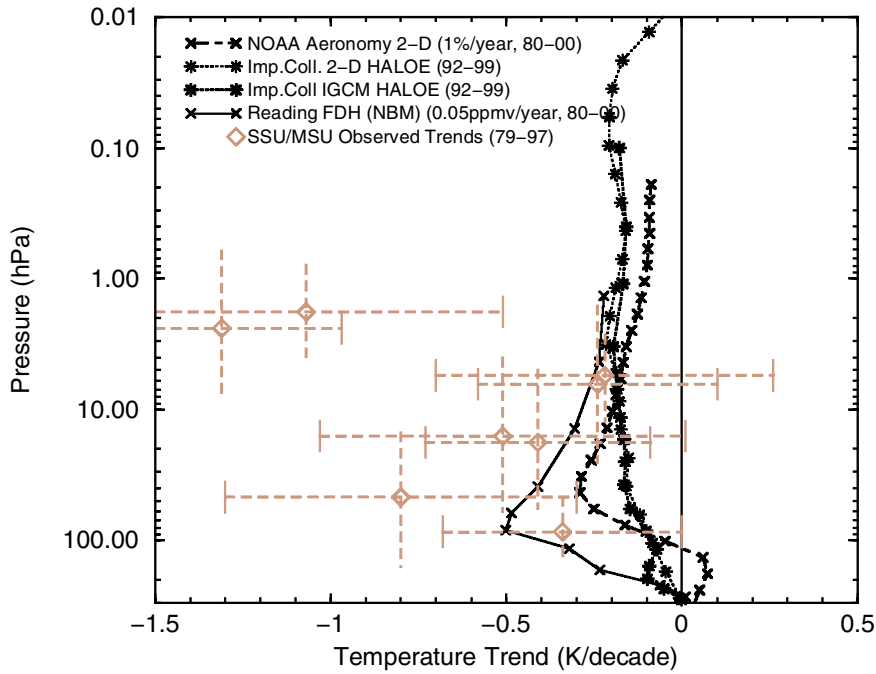

Figure 3. As Fig. 1 but using imposed water vapour trends (it is not expected that water vapour trends alone will account for the observed trends).

family schemes (Takigawa *et al.* 1999; Hein *et al.* 2001; Austin 2002; Nagashima *et al.* 2002; Schnadt *et al.* 2002). Austin *et al.* (2003) provide a detailed comparison of the results from such models at high latitudes as well as a more complete description of the models. In addition to the GCMs, temperature trends from a more traditional 2-D model (Dvortsov and Solomon 2001) with a more complete chemistry scheme are also included here.

The temperature trends from coupled-chemistry models (Fig. 4) include the impact of changing: (i) source gases (such as halocarbons) which impact on ozone directly; (ii) source gases (most importantly carbon dioxide) which are greenhouse gases (and, by changing stratospheric temperature, may change ozone indirectly); and (iii) stratospheric water vapour as it is affected by methane oxidation and stratosphere–troposphere exchange. Thus, unlike in previous subsections, the models here are attempting to include all the changes in stratospheric composition that are believed to cause stratospheric temperature trends, and so it is legitimate to compare the modelled and observed trends. Consequently, Fig. 4 includes the trends derived from radiosonde data in addition to the satellite data. The degree to which the trends with the coupled models agree with observations will be discussed in section 3(e). Note that the time period of the simulations in Fig. 4 varies. This will affect the rate of change of halogens used in the model, most notably in the CCSR/NIES model, for which the results (1986–2005) include a slight projection of trace gas trends into the future.

A significant issue with coupled-chemistry models is, of course, the degree of agreement between the model-predicted ozone change and the observed change, as this directly impacts on the quality of the modelled temperature trends. Hence it might be expected that there would be a greater degree of divergence between temperature trends in the coupled models and those models where the ozone trends are imposed.

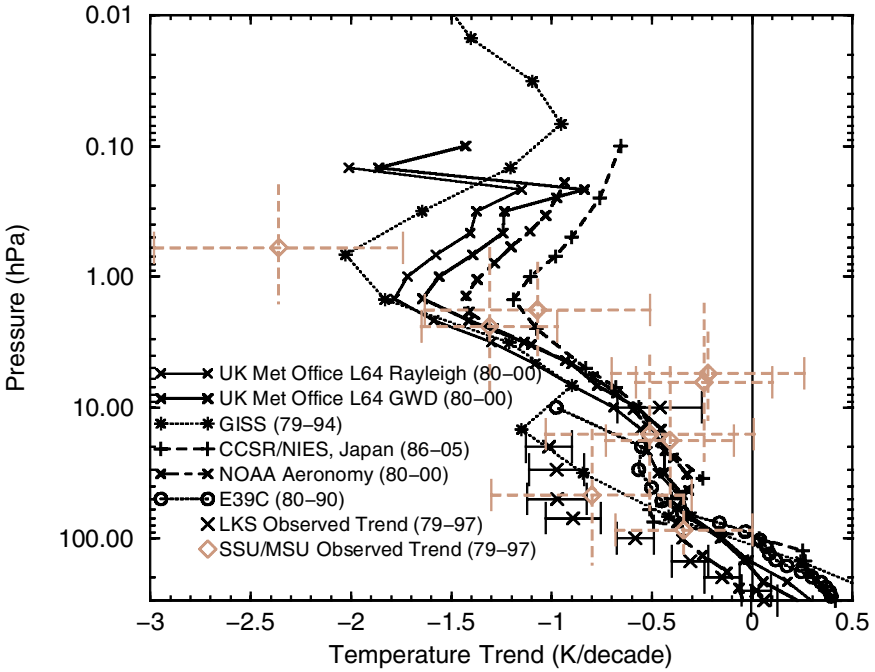

Figure 4. Global- and annual-mean temperature trends for coupled-chemistry models. The satellite trends from the Microwave Sounding Unit (MSU) and the Stratospheric Sounding Unit (SSU), and the radiosonde trends from Lanzante *et al.* (2002a,b; LKS) are also shown. The 2-sigma error bars in the observations are included; the vertical bars are intended to give the approximate altitude range sensed by the particular satellite channel. See Table 1 for details of models.

The results in Fig. 4 show that the spread, whilst considerable, is not obviously greater than the imposed ozone simulations shown in Fig. 1. It is clear though, that even in cases of reasonable agreement (e.g. between the GISS and UK Met Office runs in the upper stratosphere) there may be a difference in the causes of the total change; for the GISS and UK Met Office cases, it can be seen in Fig. 2 that the greenhouse-gas-only components are 1 K decade^{-1} different between these models.

(*e*) *Synopsis*

Figure 5 attempts to consolidate the above results for the models without interactive chemistry. The individual model results in both Figs. 1 and 2 have been averaged. For water vapour, the Imperial College IGCM HALOE trends (Fig. 3) have been adopted, as these are based on more global observations albeit for quite a short period. Summing these three components then generates the 'total' trend. This assumes that the sum of the individual components generates a cooling similar to the case when all mechanisms are included together. Both the Reading NBM FDH and an FDH model based on the E39C model show that this assumption is justified to within 1.5% for the global-mean response over the past two decades. Sexton *et al.* (2003) have also shown, in a GCM, that the temperature trend at 50 hPa is well represented by the individual components, with very little interaction between them.

Figure 5 indicates that in the region of 1 hPa, ozone and greenhouse gas changes contribute approximately equally to the cooling (about 0.8 K decade^{-1}) with water

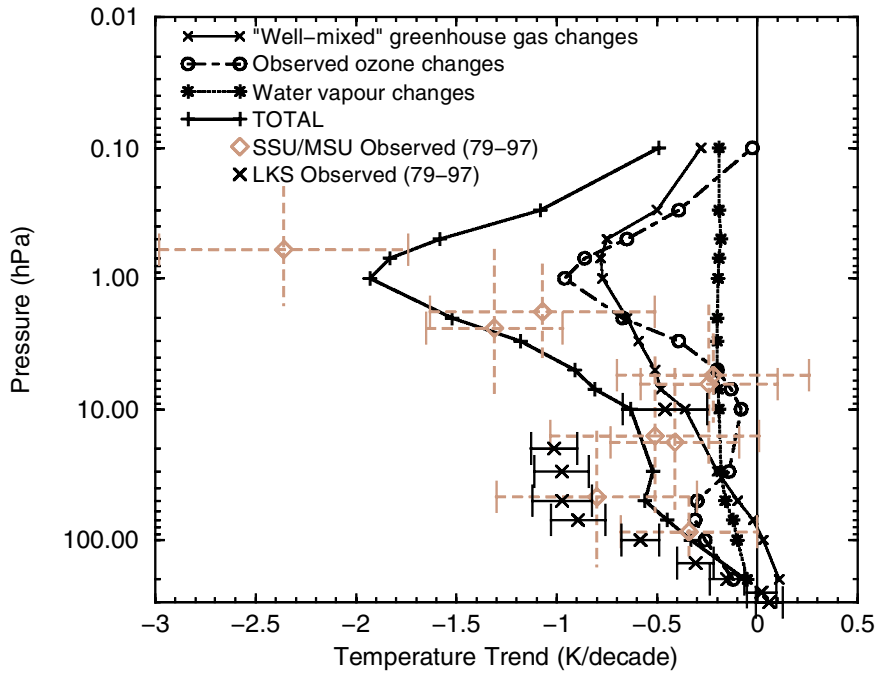

Figure 5. Global- and annual-mean temperature trends for the period approximately 1980–2000, from an average of the model results for the imposed height-resolved ozone trends (Fig. 1) and greenhouse gases (Fig. 2); the water vapour results are the Imperial College IGCM Halogen Occultation Experiment (HALOE) trends in Fig. 3. The satellite trends from the Microwave Sounding Unit (MSU) and the Stratospheric Sounding Unit (SSU), and the radiosonde trends from Lanzante *et al.* (2003a,b; LKS) are also shown. The 2-sigma error bars in the observations are included; the vertical bars are intended to give the approximate altitude range sensed by the particular satellite channel.

vapour contributing only 0.2 K decade^{-1}. It can be seen that throughout the upper stratosphere the total model cooling is within the 2-sigma error bars of the observed cooling. The ozone cooling is more strongly peaked at the stratopause than the greenhouse gas effect.

For the coupled models (Fig. 4), there is good agreement with observations at about 2 hPa, but only one of the models (the GISS model) is within the 2-sigma error bars at 0.5 hPa, with all other models generating a smaller cooling. Related to this, near 1 hPa the coupled models give a cooling in the range 1.1 to 2 K decade^{-1} (Fig. 4), and yet the mean cooling from all the processes in the uncoupled models (Fig. 5) is about 2 K decade^{-1}. Hence, the coupled models appear to be producing a generally smaller cooling than the models with imposed ozone trends. This result may be coincidental, as none of the models in which coupled-chemistry calculations were performed also contributed to the imposed-ozone comparison.

At 5–6 hPa, there is an apparently systematic disagreement with observations that has previously been noted by Austin (2002) in his coupled-chemistry GCM simulations. The total model cooling is more negative than the 2-sigma errors bars of the two SSU channels observing at these altitudes, and indeed, the contribution from greenhouse gases alone is close to the more negative end of these error bars. A similar disagreement can be seen in the coupled-model runs (Fig. 4).

The source of this discrepancy is not clear but there are a number of possibilities. First, if the minimum coolings from any of the contributing models are used (so that

ozone depletion gives zero cooling, increased greenhouse gases give a 0.45 K decade^{-1} cooling, and the water vapour cooling is less than about 0.1 K decade^{-1}) then there would be agreement within the 2-sigma error bars of the observations at 6 hPa. This might be consistent with the water vapour trend over the HALOE period at these pressures not being representative of the long-term trend. Second, there are uncertainties in the vertical profile of the changes in ozone, water vapour and, to a much lesser extent, greenhouse gases, that are imposed on the models; however, the presence of the temperature trend discrepancy in the coupled-chemistry models and the models with imposed ozone change argues against this as a major cause. Third, there may be a bias either in the satellite temperature data or the trend analysis on that data. As pointed out by Ramaswamy *et al.* (2002), the lack of any other temperature trend data to provide corroborative evidence for the SSU trends in the middle and upper stratosphere at the global scale is unfortunate; Ramaswamy *et al.* (2001) note that a variety of corrections have to be made to the SSU data that may impact on the derived trends. None of these potential explanations is compelling and so the possibility remains that the discrepancy is real, which would indicate that there is a temperature trend mechanism missing from the models.

At 10 hPa, greenhouse gases are the dominant cooling mechanism (0.4 K decade^{-1}), followed by water vapour (0.2 K decade^{-1}) with ozone causing a cooling less than 0.1 K decade^{-1}; the cooling is within the 2-sigma error bars of the radiosonde trend data, and the satellite channels at slightly lower altitudes. The majority of the coupled models (Fig. 4) are also in agreement with observations.

Between 20 and 70 hPa, the trend derived from radiosonde data is considerably more negative than that derived from the models using imposed ozone trends, by several tenths of a K decade^{-1}; the satellite data also have a more negative trend than the models although the differences are less significant. The same is generally true for the coupled models (Fig. 4) with the exception of the GISS model at 20–30 hPa. As noted in section 2, data quality remains a significant issue in understanding differences between models and observations, as there is evidence that the sonde-based trend estimates are too negative in the tropics and this will impact on the global mean. Nonetheless, assuming that at least some part of this discrepancy is real, one possible explanation is stratospheric water vapour changes. Figure 3 indicates that an extra cooling of a few tenths of a K decade^{-1} would result if the Boulder sonde-based water vapour trends were used rather than the HALOE water vapour trends. If this were one explanation for the model–observation difference, water vapour could dominate over ozone as the main cause of temperature trends in this altitude region.

At 100 hPa, ozone is again the dominant cooling mechanism (around 0.3 K decade^{-1}) with water vapour giving a cooling of 0.1 K decade^{-1} and the greenhouse gases giving near-zero cooling. The net cooling is close to that derived from the MSU observations, but the sonde data give a significantly larger cooling, which may also be consistent with a larger water vapour contribution. The MSU data, as it samples the tropical upper troposphere, may be underestimating the stratospheric cooling, but likewise there are concerns about the quality of the sonde-based estimates, although these have a superior vertical resolution.

4. Zonal- and annual-mean trends in the lower stratosphere

(*a*) *Variability*

In the global- and annual-mean cases in section 3, the variability of modelled temperatures is small compared both to the observed trends and to some of the intermodel

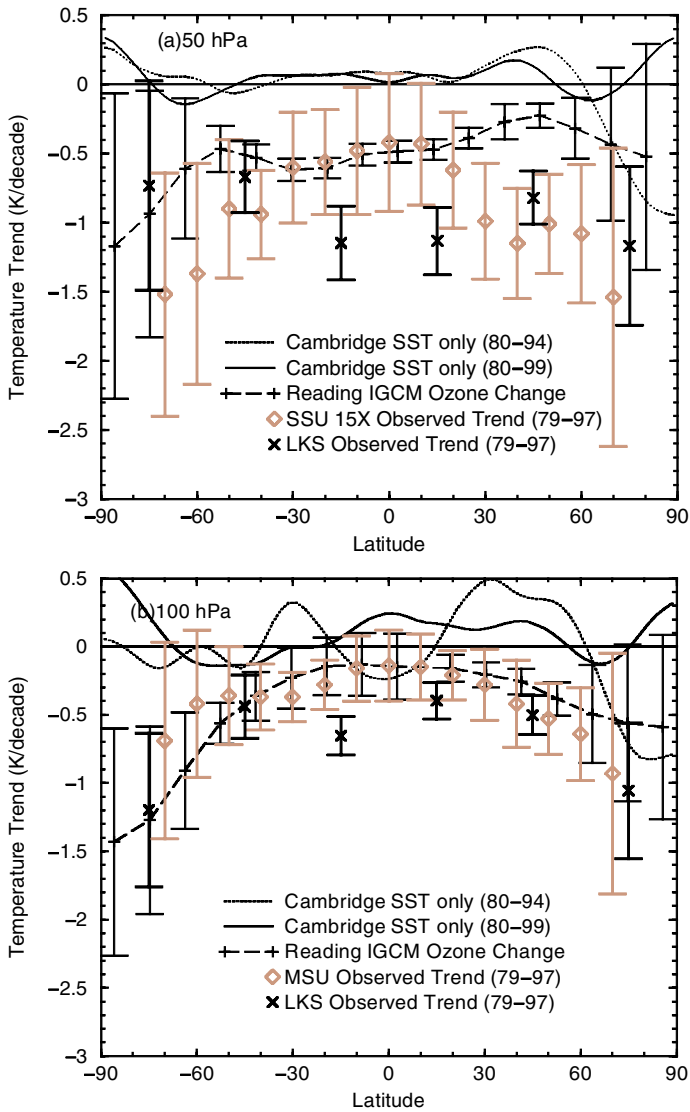

Figure 6. Annual- and zonal-mean temperature trends at (a) 50 hPa and (b) 100 hPa. The trends from the Stratospheric Sounding Unit (SSU) channel 15X, Microwave Sounding Unit (MSU) channel 4 and the Lanzante *et al.* (2003a,b; LKS) data are also shown. The 2-sigma error bars in the observation are included. The peak of SSU channel 15X weighting function in (a) is at about 46 hPa. The peak of the MSU channel 4 weighting function in (b) is at about 86 hPa. The LKS radiosonde data represent 30° latitude bands centred on the plotted symbol. The trends from the Cambridge model, which is forced only by SST variations, are shown for two different periods. Another measure of unforced variability is indicated by the 2-sigma standard error derived from the Reading IGCM, shown superimposed on the imposed ozone trend calculations; for clarity, the Reading data are only plotted at every other latitude. See Table 1 for details of models.

differences, and it was relatively easy to assign significance both to the trends and to some of the differences. For the zonal-mean trends the variability is much larger, and the significance of the modelled trends and the differences both between models and with observations is harder to establish.

Figure 6 shows an attempt to characterize the variability in different ways at 50 and 100 hPa. The plots show both the satellite- and radiosonde-derived trends and the

associated ±2-sigma uncertainty in the trend estimate. Figure 6 also shows the linear trends derived by Cambridge for two different periods, using a GCM run with observed time-varying SSTs but no imposed changes in trace gas concentrations. Finally, it shows the ±2-sigma standard error from a 30-year control run of the Reading IGCM, plotted relative to the trend from the imposed ozone change runs for reference.

At 50 hPa (Fig. 6(a)) in southern and northern midlatitudes, the modelled and observed trends are generally larger than the trends from the model forced with only SST variations. In high latitudes both the modelled and observed variability increase markedly, indicating the need for caution in ascribing trends to particular causes. Near the equator, the cooling trends derived from the satellite data are only marginally significantly different from zero; the trends derived from radiosonde data are significantly more negative but, as discussed in section 2, there are concerns about the reliability of the data in this region. The absence of a quasi-biennial oscillation in the GCMs may mean that the model variability in the tropics is underestimated.

At 100 hPa (Fig. 6(b)), in both the tropics and northern high latitudes, the magnitude of the modelled trends forced with only SST variations is large, as is the uncertainty in the observed trend estimates and the size of the model standard error. This clearly precludes any confident attempt to attribute the observed cooling to any trends in trace gas changes in these regions; the size of the negative trend from the radiosonde data in the southern tropics is notable but should again be the subject of caution. In midlatitudes of both hemispheres and at southern high latitudes for the radiosonde data, there is a clearer separation of the observed trends from zero, as there is for the Reading IGCM temperature trends using imposed ozone changes. This indicates that a trend attribution in these regions may be possible, although the size of the unforced modelled trends indicates that some caution is needed in interpretation.

(*b*) *Simulated temperature trends using observed ozone trends*

Figure 7 shows the annual- and zonal-mean trends at 50 and 100 hPa due to imposed ozone changes alone. At 50 hPa (Fig. 7(a)), the general pattern in the GCMs is of a cooling of a few tenths of a K decade^{-1} in low latitudes. With the exception of the GFDL GCM, there is considerably less latitudinal gradient in the temperature trend in the southern hemisphere in the GCMs compared to the FDH models; as discussed in Rosier and Shine (2000), changes in the model circulation tend to ameliorate the radiatively driven high-latitude cooling. For the three GCMs in Fig. 7(a), the intermodel difference is smaller than the model variability shown in Fig. 6(a) in high latitudes and northern midlatitudes; in the tropics and southern midlatitudes it is larger. This indicates that some features of the models (such as their radiation or gravity-wave drag schemes, or dynamical response to the change in diabatic heating) or the implementation of the ozone trends is causing their responses to differ significantly.

At 100 hPa (Fig. 7(b)) the GCMs are in better agreement, and the separation between GCMs and FDH models is clearer. In midlatitudes, a cooling trend of around 0.3 K decade^{-1} is seen in the models and the differences amongst the GCMs is no larger than the model variability shown in Fig. 6(b).

(*c*) *Simulated temperature trends due to increased greenhouse gas concentrations*

For the greenhouse gases, Fig. 8 indicates in most models near-zero cooling at all latitudes at 100 hPa, and around 0.1 K decade^{-1} cooling at 50 hPa. The response of the GISS GCM is quite different from the other GCMs, giving a considerably higher cooling at higher latitudes and a warming in low latitudes. This is a signature of a slowing of the

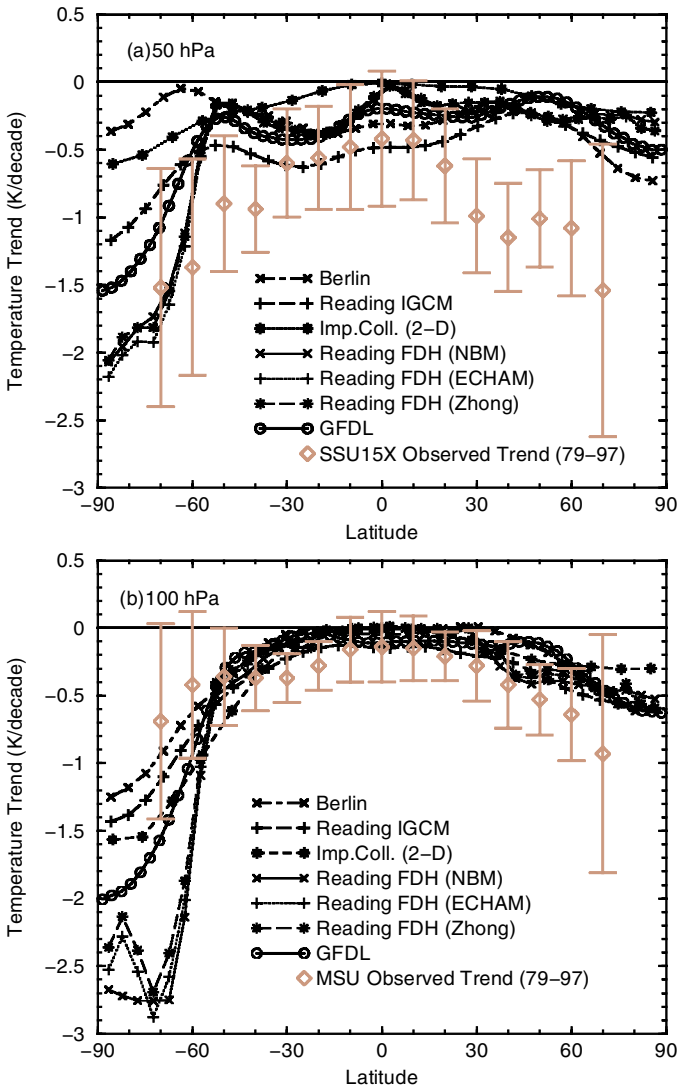

Figure 7. Annual- and zonal-mean temperature trends at (a) 50 hPa and (b) 100 hPa for models using imposed height-resolved ozone trends. The trends from the Stratospheric Sounding Unit (SSU) channel 15X and Microwave Sounding Unit (MSU) channel 4 are also shown. The 2-sigma error bars in the observation are included. The peak of the SSU channel 15X weighting function in (a) is at about 46 hPa. The peak of the MSU channel 4 weighting function in (b) is at about 86 hPa. Note that the observations are shown here for reference, but it is not expected that ozone trends alone will account for the observed trends. See Table 1 for details of models.

meridional circulation resulting from a difference in the interaction of waves with the mean flow when carbon dioxide is increased. As with the impact of the observed ozone trends, the intermodel differences are similar to the model variability at 100 hPa, but at low and middle latitudes exceed the model variability at 50 hPa.

(*d*) *Simulated temperature trends due to trends in stratospheric water vapour*

For the changes in stratospheric water vapour, the zonal-mean trends at 50 and 100 hPa (Fig. 9) reflect the divergence indicated in the annual-mean results (section 3(c)), due to the uncertainties in knowledge of the actual change in water vapour

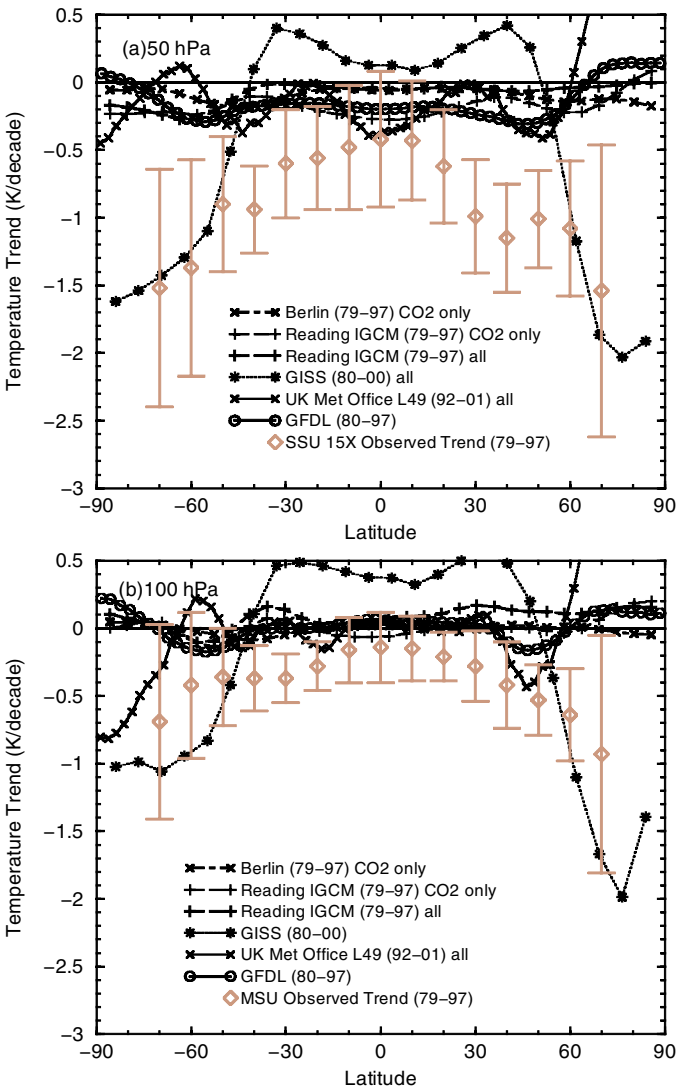

Figure 8. Annual- and zonal-mean temperature trends at (a) 50 hPa and (b) 100 hPa for models using imposed changes in greenhouse gas concentrations. The trends from the Stratospheric Sounding Unit (SSU) channel 15X and Microwave Sounding Unit (MSU) channel 4 are also shown. The 2-sigma error bars in the observation are included. The peak of the SSU channel 15X weighting function in (a) is at about 46 hPa. The peak of the MSU channel 4 weighting function in (b) is at about 86 hPa. Note that the observations are shown here for reference, but it is not expected that greenhouse gas trends alone will account for the observed trends. See Table 1 for details of models.

concentrations. At 50 hPa, the models with the more idealized water vapour changes (NOAA and Reading) generate extratropical coolings of 0.3 to 0.6 K decade^{-1}, with the Imperial College IGCM runs using HALOE data generating similar coolings in high southern latitudes.

(*e*) *Simulated temperature trends from coupled-chemistry models*

Figure 10 shows the zonal-mean trends at 50 and 100 hPa for the coupled-chemistry models; since these models attempt to include all trend mechanisms considered here, it

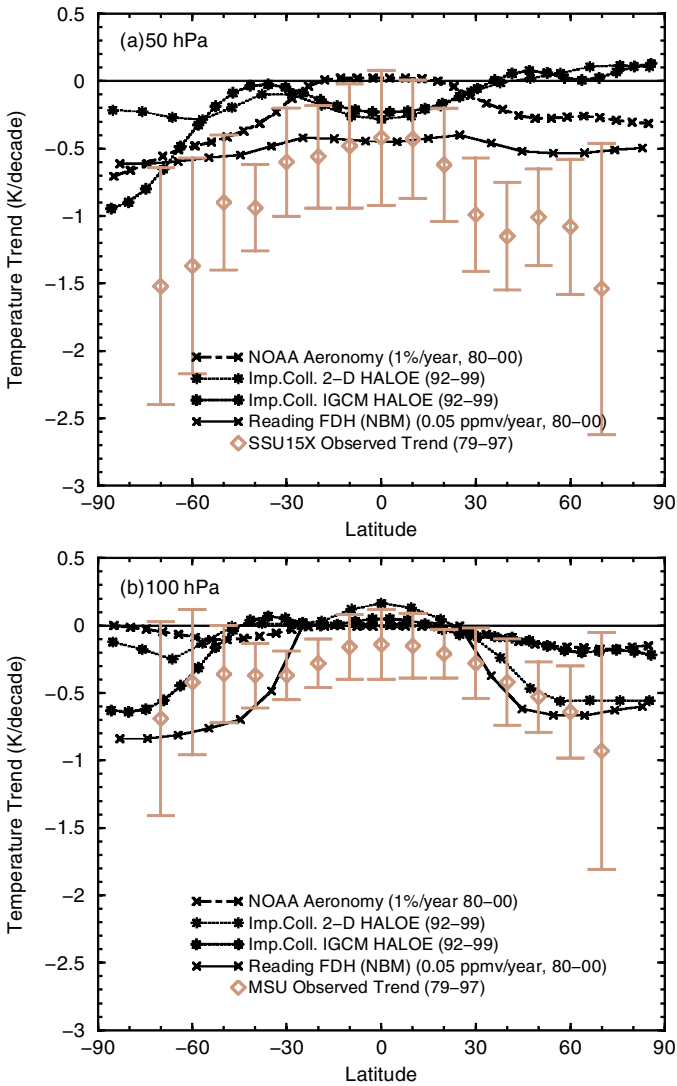

Figure 9. Annual- and zonal-mean temperature trends at (a) 50 hPa and (b) 100 hPa for models using imposed changes in stratospheric water vapour. The trends from Stratospheric Sounding Unit (SSU) channel 15X and Microwave Sounding Unit (MSU) channel 4 are also shown. The 2-sigma error bars in the observation are included. The peak of the SSU channel 15X weighting function in (a) is at about 46 hPa. The peak of the MSU channel 4 weighting function in (b) is at about 86 hPa. Note that the observations are shown here for reference, but it is not expected that water vapour trends alone will account for the observed trends. See Table 1 for details of models.

is legitimate to compare these trends with the observations, but this discussion is delayed until the next subsection.

At 50 hPa (Fig. 10(a)), throughout the tropics and midlatitudes, there is a spread in the derived cooling rates of order 0.5 K decade^{-1}, although the average is a cooling of around 0.25 K decade^{-1}. Only in southern high latitudes is there better agreement, with all GCMs generating a cooling in the range 1 to 2 K decade^{-1}

The situation is similar at 100 hPa (Fig. 10(b)). There is a considerable spread amongst the models, and within the tropics there is no consensus on even the sign of the

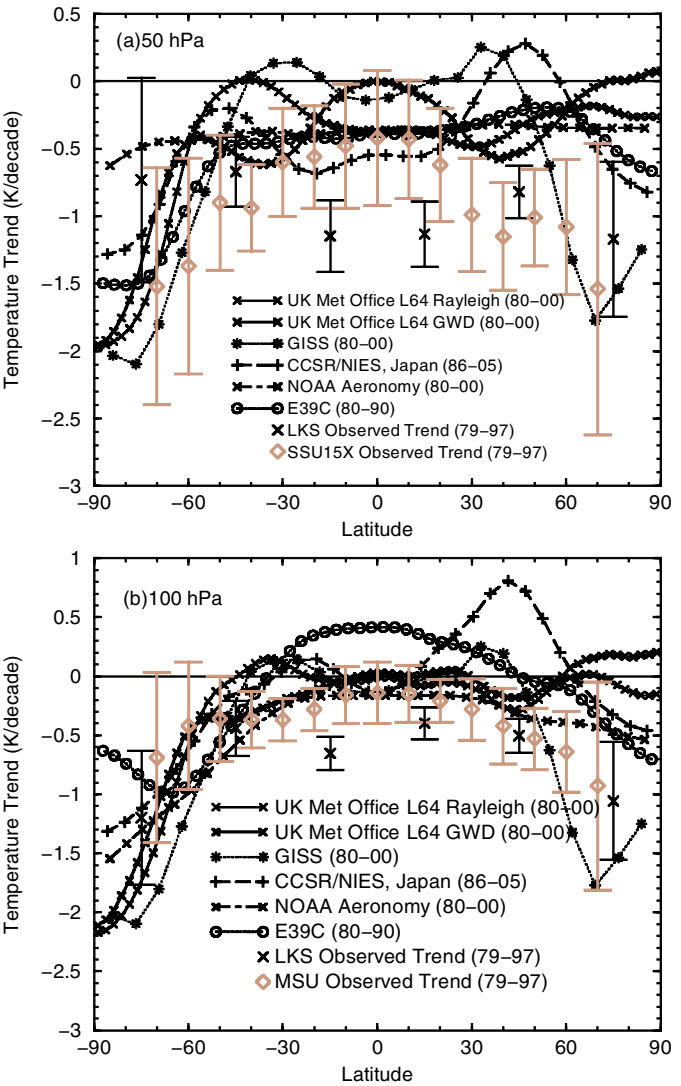

Figure 10. Annual- and zonal-mean temperature trends at (a) 50 hPa and (b) 100 hPa for the coupled-chemistry models. The trends from Stratospheric Sounding Unit (SSU) channel 15X and Microwave Sounding Unit (MSU) channel 4 and the Lanzante *et al.* (2003a,b; LKS) radiosonde data are also shown. The 2-sigma error bars in the observation are included. The peak of the SSU channel 15X weighting function in (a) is at about 46 hPa. The peak of the MSU channel 4 weighting function in (b) is at about 86 hPa. The LKS radiosonde data represent 30° latitude bands centred on the plotted symbol. See Table 1 for details of models.

temperature trend. It is only in southern high latitudes that the models all show a marked cooling.

(*f*) *Synopsis*

In the tropics at 50 hPa, the majority of the models and all the GCMs with imposed ozone trends (Fig. 7(a)) are within the 2-sigma error bars of the satellite trends, indicating that the approximately 0.3 K decade^{-1} cooling due to ozone change alone could explain these observations. However, most models give a smaller cooling than the

satellite data, and a much smaller cooling than the radiosonde data (which may be less reliable in this region) shown in Fig. 6(a). Given the size of the observational uncertainty, changes in greenhouse gases and, with less certainty, stratospheric water vapour changes could each add about 0.2 K decade^{-1} cooling at 50 hPa without disrupting the agreement with the satellite observations. The model trends could be made more consistent with the radiosonde trends, either by taking the extreme coolings amongst the models for the imposed ozone and greenhouse gas cases, together with the coolings derived from the HALOE water vapour trends, or else by taking the mid-range estimates of the ozone and greenhouse gas cases and the more extreme water vapour coolings simulated by the Reading NBM FDH (Fig. 9(a)). The coupled models (Fig. 10(a)) are in better agreement with satellite-derived trends in the tropics, although the majority of the models also give a somewhat smaller cooling.

At 50 hPa in midlatitudes of both hemispheres, there is good agreement between the satellite- and radiosonde-derived trends (Fig. 6(a)), but a substantial difference between the ozone-induced trends from the models (Fig. 7(a)) and the observations, most notably in the northern hemisphere. The radiosonde trend using the Freie Universität Berlin stratospheric analyses for the slightly longer period of 1979–2000 (Ramaswamy *et al.* 2002) also agrees well with the other trend sources in Fig. 6(a); hence the discrepancy is not being greatly affected by the series of cold northern winters in the early 1990s. Figure 6(a) shows a clear separation between the Reading IGCM error bars and the observations. At 40°N the gap between the mean of the models and the mid-point of the cooling is about 1 K decade^{-1} (even the extreme of the observed error bar differs from the models by around 0.5 K decade^{-1}). This difference is much more than can be explained by greenhouse gas changes alone (most models report a cooling of about 0.2 K decade^{-1}, although two models report 0.4 K decade^{-1}).

To test whether this underestimate of the observed midlatitude cooling is significant, given the large uncertainties, we used a modified Student's t test, which accounts for unequal variances (von Storch and Zwiers 1999) to examine the differences between the GCM results and satellite-derived trends at 50 hPa. Using a standard deviation of 0.2 K decade^{-1} derived from the spread of model results and a similar uncertainty for the observed trends, indicates significant differences (at the 95% confidence level) for an individual latitude between 30 and 50°N. Incorporating the results from neighbouring latitudes and 100 hPa dramatically improves this significance to over 99.99%, even when allowing for a degree of dependence between results at different latitudes and pressures. Therefore, it can be stated with some confidence that the models with imposed ozone and greenhouse gas changes underestimate the observed lower-stratosphere cooling in the northern midlatitudes.

Just to bring the models within the 2-sigma error bars of the observations would need a cooling of around 0.3 K decade^{-1} from other mechanisms in addition to ozone and greenhouse gas change. To achieve the observed cooling at 40°N (about 1.2 K decade^{-1}) would require a much larger additional cooling contribution, of around 0.7 K decade^{-1}. Water vapour trends could explain much of the discrepancy, but it would require trends in excess of those deduced from HALOE and more consistent with the trends used in the Reading NBM FDH calculations (50 ppbv year^{-1}). Such a trend would also improve agreement at 50 hPa in the global- and annual-mean plot (Fig. 5). It is also of note that none of the coupled-chemistry models (Fig. 10(a)) lies within the 2-sigma bars of the observations between 30° and 50°N.

It is at precisely these latitudes that sonde observations (albeit at a single location) indicate large stratospheric water vapour trends sustained over two decades (see subsection 3(c)), which supports the argument that water vapour is a major contributor

to the difference. However, water vapour is only one potential reason for the discrepancy, which could also be due to either interannual variability that is not sampled by the models or a long-term dynamical trend. Observed decreases in planetary-wave driving between 1979 and 2000 (Newman and Nash 2000; Randel *et al.* 2002) are consistent with at least some fraction of the northern hemisphere midlatitude cooling being due to dynamics.

At high northern latitudes, there is a tendency for the models with imposed ozone trends alone (Fig. 7(a)), and many of the coupled models (Fig. 10(a)), to underestimate the observed cooling by of order 1 K decade^{-1}. Contributions from greenhouse gases and water vapour would reduce this difference but given the large model variability (Fig. 6(a)) it is difficult to be conclusive. However, at high southern latitudes, the coupled-chemistry models (see Fig. 10(a)) are in generally better agreement with observations, as are two of the three GCMs with imposed ozone (Fig. 7(a)).

For the zonal-average trends at 100 hPa, Figs. 6(b) and 7(b) indicate that ozone depletion alone can explain the observed trends at all latitudes, as the error bars of the satellite and models overlap. The greenhouse gas trend is small, and a cooling due to water vapour of several tenths K decade^{-1} could be present; this would improve the midlatitude agreement with the observed temperature trend, particularly for those models in Fig. 7(b) with smaller ozone-induced cooling. The satellite and radiosonde trends agree well except, as noted earlier, in the southern tropics. The coupled models (Fig. 10(b)) indicate a considerably greater spread in low and midlatitude temperature trends and a tendency, if anything, for the models to underestimate the observed cooling.

5. Conclusions

There is strong evidence that the stratosphere has cooled over recent decades, and models are able to reproduce the general features of the vertical profile of the observed global- and annual-mean cooling. This allows a general picture of the contributions to the trend to be built up. In the upper stratosphere, ozone and greenhouse gas changes contribute approximately equally; in the lower stratosphere, ozone depletion is a major contributor. But the quantitative degree of agreement is not always good. At 5 to 6 hPa, the models give a consistently stronger cooling trend than the satellite data, which provide the only available global temperature trend series at these pressures. The degree of disagreement depends on how important the cooling trend due to stratospheric water vapour changes are at these pressures. It has not been possible to ascribe a cause to this; it may be due to missing mechanisms in the models or to a problem with the data on which trend analyses are performed. Between 20 and 70 hPa, particularly when comparing models and radiosonde trends, the modelled cooling is smaller than that observed. The difference is consistent with a large cooling trend due to increases in stratospheric water vapour, but current observations on the global nature of those increases are not adequate to be conclusive.

For the zonal- and annual-mean trends at 50 hPa and 100 hPa, the evidence is that ozone depletion is a major contributor to the trends. The most significant disagreement between models and observations is in the northern midlatitudes at 50 hPa, where the mean observed cooling is up to 1 K decade^{-1} larger than the mean cooling of the models using ozone trends alone imposed from observations. Again trends in stratospheric water vapour are one potential explanation. However, contributions from other sources, such as trends in dynamical forcing, cannot be ruled out.

There is also a significant spread amongst the models, which is particularly worrying in cases with relatively well-defined perturbations to the trace gas fields (such as ozone and greenhouse gases). There are a number of potential sources for the divergence amongst the models, which would require further study to establish. For the global-mean differences, the most obvious explanation is differences between the responses of individual radiation schemes to changes in constituents. It has also been shown in earlier work that, for both water vapour and ozone perturbations, the differences in the baseline from which those perturbations are made can lead to significant differences in model response. For the zonal-mean differences, the different sensitivities in the dynamical forcing in the models to changes in trace gases might also be important. An important issue for the coupled-chemistry models is the degree of agreement between predicted ozone changes, both amongst the models and with observations. Comparisons have been performed for high latitudes (Austin *et al.* 2003); however, the spread in the temperature trends from the coupled-chemistry models and the apparently smaller total cooling in the upper stratosphere compared to the imposed ozone trend calculations, indicate the need for a similar exercise for global ozone. Some of these issues fall within the remit of an existing stratospheric model-evaluation exercise (Pawson *et al.* 2000).

It is also clear that a full assessment of the causes of stratospheric temperature trends is seriously hampered by uncertainties in the analysis of observations both of the temperatures and of the radiatively active gases that are important for determining the temperature.

Acknowledgements

KPS, MSB and SHEH thank NERC for support (GST022385 and NER/T/S/2002/00058). PMdeFF is funded by a NERC Advanced Fellowship. DTS thanks NASA's Atmospheric Chemistry Modelling and Analysis Program for support. CAS was funded by a NERC studentship. JA and NB were supported by the European Framework 5 project EuroSPICE, the UK Department for the Environment, Food and Rural Affairs and the UK Government Meteorological Research Programme. UL thanks the German Ministry for Education and research for financial support (Grant 01LO9511/8) and Konrad-Zuse-Zentrum für Informationstechnik Berlin for providing computer resources.

References

Austin, J. 2002 A three-dimensional coupled chemistry–climate model simulation of past stratospheric trends. *J. Atmos. Sci.*, **59,** 218–232

Austin, J., Shindell, D., Beagley, S. R., Brühl, C., Dameris, M., Manzini, E., Nagashima, T., Newman, P., Pawson, S., Pitari, G., Rozanov, E., Schnadt, C. and Shepherd, T. G. 2003 Assessments of chemistry–climate models of the stratosphere. *Atmos. Chem. Phys. Discuss.*, **3,** 1–27

Braesicke, P. and Pyle, J. A. 2003 Changing ozone and changing circulation in northern mid-latitudes: Possible feedbacks? *Geophys. Res. Lett.*, **30,** 1059, doi: 10.1029/2002GL015973

Butchart, N., Austin, J., Knight, J. R., Scaife, A. A. and Gallani, M. L. 2000 The response of the stratospheric climate to projected changes in the concentrations of well-mixed greenhouse gases from 1992 to 2051. *J. Climate*, **13,** 2142–2159

Dvortsov, V. L. and Solomon, S. 2001 Response of the stratospheric temperatures and ozone to past and future increases in stratospheric humidity. *J. Geophys. Res.-Atmos.*, **106,** 7505–7514

Forster, P. M. D. and Shine, K. P. 1999 Stratospheric water vapour changes as a possible contributor to observed stratospheric cooling. *Geophys. Res. Lett.*, **26,** 3309–3312

Forster, P. M. D., Freckleton, R. S. and Shine, K. P. 1997 On aspects of the concept of radiative forcing. *Clim. Dyn.*, **13,** 547–560

Forster, P. M. D., Ponater, M. and Zhong, W. Y. 2001 Testing broadband radiation schemes for their ability to calculate the radiative forcing and temperature response to stratospheric water vapour and ozone changes. *Meteorol. Z.*, **10,** 387–393

Forster, P. M. de F. and Shine, K. P. 2002 Assessing the climate impact of trends in stratospheric water vapor. *Geophys. Res. Lett.*, **29,** doi: 10.1029/2001GL013909

Hein, R., Dameris, M., Schnadt, C., Land, C., Grewe, V., Kohler, I., Ponater, M., Sausen, R., Steil, B., Landgraf, J. and Brühl, C. 2001 Results of an interactively coupled atmospheric chemistry–general circulation model: Comparison with observations. *Ann. Geophys.*, **19,** 435–457

Langematz, U. 2000 An estimate of the impact of observed ozone losses on stratospheric temperature. *Geophys. Res. Lett.*, **27,** 2077–2080

Langematz, U., Kunze, M., Krüger, K., Labitzke, K. and Roff, G. L. 2003 Thermal and dynamical changes of the stratosphere since 1979 and their link to ozone and CO_2 changes. *J. Geophys. Res.*, **108,** 4027, doi: 1029/2002JD002069

Lanzante, J. R., Klein, S. A. and Seidel, D. J. 2003a Temporal homogenization of monthly radiosonde temperature data. Part I: Methodology. *J. Climate*, **16,** 224–240

2003b Temporal homogenization of monthly radiosonde temperature data. Part II: Trends, sensitivities and MSU comparisons. *J. Climate*, **16,** 241–262

Nagashima, T., Takahashi, M., Takigawa, M., and Akiyoshi, H. 2002 Future development of the ozone layer calculated by a general circulation model with fully interactive chemistry. *Geophys. Res. Lett.*, **29,** 10.1029/2001GL014026

Nash, J. and Forrester, G. F. 1986 Long-term monitoring of stratospheric temperature trends using radiance measurements obtained by the TIROS-N series of NOAA spacecraft. *Adv. Space. Res.*, **6,** 37–44

Newman, P. A. and Nash, E. R. 2000 Quantifying the wave driving in the stratosphere. *J. Geophys. Res.*, **105,** 12485–12497

Oinas, V., Lacis, A. A., Rind, D., Shindell, D. T. and Hansen, J. E. 2001 Radiative cooling by stratospheric water vapor: Big differences in GCM results. *Geophys. Res. Lett.*, **28,** 2791–2794

Oltmans, S. J., Vomel, H., Hofmann, D. J., Rosenlof, K. H. and Kley, D. 2000 The increase in stratospheric water vapor from balloon-borne frostpoint hygrometer measurements at Washington, DC, and Boulder, Colorado. *Geophys. Res. Lett.*, **27,** 3453–3456

Pawson, S., Kodera, K., Hamilton, K., Shepherd, T. G., Beagley, S. R., Boville, B. A., Farrara, J. D., Fairlie, T. D. A., Kitoh, A., Lahoz, W. A., Langematz, U., Manzini, E., Rind, D. H., Scaife, A. A., Shibata, K., Simon, P., Swinbank, R., Takacs, L., Wilson, R. J., Al-Saadi, J. A., Amodei, M., Chiba, M., Coy, L., de Grandpre, J., Eckman, R. S., Fiorino, M., Grose, W. L., Koide, H., Koshyk, J. N., Li, D., Lerner, J., Mahlman, J. D., McFarlane, N. A., Mechoso, C. R., Molod, A., O'Neill, A., Pierce, R. B., Randel, W. J., Rood, R. B. and Wu, F. 2000 The GCM–reality intercomparison project for SPARC (GRIPS): Scientific issues and initial results. *Bull. Am. Meteorol. Soc.*, **81,** 781–796

Ramaswamy, V. and Schwarzkopf, M. D. 2002 Effects of ozone and well-mixed gases on annual-mean stratospheric temperature trends. *Geophys. Res. Lett.*, **29,** 2064:10.1029/2002GL015141

Ramaswamy, V., Schwarzkopf, M. D. and Randel, W. 1996 Fingerprint of ozone depletion in the spatial and temporal patterns of recent lower stratospheric cooling. *Nature*, **382,** 616–618

Ramaswamy, V., Chanin, M. L., Angell, J., Barnett, J., Gaffen, D., Gelman, M., Keckhut, P., Koshelkov, Y., Labitzke, K., Lin, J. J. R., O'Neill, A., Nash, J., Randel, W., Rood, R., Shine, K., Shiotani, M. and Swinbank, R. 2001 Stratospheric temperature trends: Observations and model simulations. *Rev. Geophys.*, **39,** 71–122

Ramaswamy, V., Gelman, M. E., Schwarzkopf, M. D. and Lin, J.-J. R. 2002 'An update of stratospheric temperature trends'. Pp. 7–9 in SPARC Newsletter No. 18, Météo-France, Toulouse, France

Randel, W. J. and Cobb, J. B. 1994 Coherent variations of monthly mean total ozone and lower stratospheric temperature. *J. Geophys. Res.*, **100,** 5443–5447

Randel, W. J. and Wu, F. 1999 A stratospheric ozone trends data set for global modelling studies. *Geophys. Res. Lett.*, **26,** 3089–3092

Randel, W. J., Wu, F. and Stolarski, R. 2002 Changes in column ozone correlated with the stratospheric EP flux. *J. Meteorol. Soc. Jpn*, **80,** 849–862

Rosenlof, K. H., Oltmans, S. J., Kley, D., Russell, J. M., Chiou, E. W., Chu, W. P., Johnson, D. G., Kelly, K. K., Michelsen, H. A., Nedoluha, G. E., Remsberg, E. E., Toon, G. C. and McCormick, M. P. 2001 Stratospheric water vapor increases over the past half-century. *Geophys. Res. Lett.*, **28,** 1195–1198

Rosier, S. M. and Shine, K. P. 2000 The effect of two decades of ozone change on stratospheric temperatures as indicated by a general circulation model. *Geophys. Res. Lett.*, **27,** 2617–2620

Schnadt, C., Dameris, M., Ponater, M., Hein, R., Grewe, V. and Steil, B. 2002 Interaction of atmospheric chemistry and climate and its impact on stratospheric ozone. *Clim. Dyn.*, **18,** 501–517

Sexton, D. M. H., Grubb, H., Shine, K. P. and Folland, C. K. 2003 Design and analysis of climate model experiments for the efficient estimation of anthropogenic signals. *J. Climate*, in press

Shindell, D. T. 2001 Climate and ozone response to increased stratospheric water vapor. *Geophys. Res. Lett.*, **28,** 1551–1554

Shindell, D. T. and Grewe, V. 2002 Separating the influence of halogen and climate changes on ozone recovery in the upper stratosphere. *J. Geophys. Res.*, **107,** 10.1029/2001JD000420

Smith, C. A. 2001 Radiative effects of observed trends in stratospheric water vapour, PhD Thesis, Imperial College, London

Smith, C. A., Haigh, J. D. and Toumi, R. 2001 Radiative forcing due to trends in stratospheric water vapour. *Geophys. Res. Lett.*, **28,** 179–182

Spencer, R. W. and Christy, J. R. 1993 Precision lower stratospheric temperature monitoring with the MSU technique: Validation and results 1979–91. *J. Climate*, **6,** 1191–1204

Takigawa, M., Takahashi, M. and Akiyoshi, H. 1999 Simulation of ozone and other chemical species using a Center for Climate System Research/National Institute for Environmental Studies atmospheric GCM with coupled chemistry. *J. Geophys. Res.-Atmos.*, **104,** 14003–14018

von Storch, H. and Zwiers, F. W. 1999 *Statistical analysis in climate research*. Cambridge University Press, Cambridge, UK

WMO 1999 'Scientific Assessment of Ozone Depletion: 1998'. Global Ozone Research and Monitoring Project Report No 44. World Meteorological Organization, Geneva, Switzerland

2003 'Scientific Assessment of Ozone Depletion: 2002'. Global Ozone Research and Monitoring Project Report No 47. World Meteorological Organization, Geneva, Switzerland